Earth and Planetary Science Letters, 104 (1991) 226–244
Elsevier Science Publishers B.V., Amsterdam

[XLeP]

Astronomical calibration of Gauss to Matuyama sapropels in the Mediterranean and implication for the Geomagnetic Polarity Time Scale

F.J. Hilgen

Department of Geology, Institute of Earth Sciences, Budapestlaan 4, 3584 CD Utrecht, The Netherlands

Received July 26, 1990; revision accepted March 1, 1991

ABSTRACT

The late Pliocene–early Pleistocene sapropel-bearing sequences exposed in the Vrica, Semaforo, Singa and Punta Piccola sections of southern Italy and the Francocastello section on Crete have been calibrated to the new astronomical solutions for the precession of the equinox and the eccentricity of the Earth's orbit using inferred phase relationships between these orbital cycles and the sapropel cycles. A new Mediterranean Precession-Related Sapropel (MPRS) coding is introduced according to which sapropels are coded after the correlative peak of the precession index as numbered from the Recent. These sapropels can now be dated with an accuracy of 1 ka by taking a time lag of 4 ka between orbital forcing, and maximum climate response and sapropel formation into account.

This tuning further results in ages for the Pliocene–Pleistocene boundary (1.81 Ma), the top of the Olduvai (1.79 or 1.84), the bottom of the Olduvai (1.95 ± 0.01), the Reunion (2.14–2.15), the Gauss/Matuyama (2.59/2.62) and the top of the Kaena (3.02 ± 0.01). These ages are remarkably similar to the astronomically calibrated ages obtained independently by Shackleton et al. based on ODP Site 677 ([1], Trans. R. Soc. Edinb., 81, 1990), but deviate considerably from those provided by Ruddiman et al. ([2], Paleoceanography, Vol. 4) and Raymo et al. based on DSDP Site 607 ([3], Paleoceanography, Vol. 4). The constant discrepancy of 130 ka with the time scale of Ruddiman et al. and Raymo et al. is explained by the new age of 0.78 instead of 0.73 Ma for the Brunhes/Matuyama, as recently proposed by Shackleton et al., and the fact that Ruddiman et al. missed two obliquity related cycles in the Brunhes/Matuyama to top Olduvai interval. Our astronomically calibrated ages do not confirm the conventional radiometric ages of the reversal boundaries, but, on the contrary, imply that K/Ar radiometric dating yields ages that are consistently too young by 5–7%.

1. Introduction

The Olduvai Subchron was originally defined as the event of normal polarity within the reversed Matuyama Chron, which was recorded in basalts and tuffs intercalated in the basal part of the sedimentary succession in the Olduvai Gorge in Tanzania [4,5]. Based on numerous radiometric (K/Ar) datings from different localities, it is presently assumed that the Olduvai Subchron lasted from 1.87 to 1.67 Ma [6]. By approximation, these ages also appear in widely used polarity time scales which are essentially based on linear interpolation between radiometrically dated age calibration points in marine magnetic anomaly sequences [7,8].

At present, an alternative method is being developed which can be used to assign absolute ages to geomagnetic polarity reversals, i.e. the tuning of proxy records climatic to the astronomical solutions for the variations in the Earth's orbit. The primary goal of these tuning procedures was to evaluate the orbital theory of the Pleistocene ice ages and to develop a high-resolution time scale for the last 780,000 years [9]. At the same time, this tuning procedure may provide very accurate, absolute ages for polarity reversals if a detailed magnetostratigraphy of these proxy records can be determined. This tuning is already well established for records spanning the last 700,000 years [9–12], and application of this procedure to immediately older sequences yielded ages for the reversal

0012-821X/91/$03.50

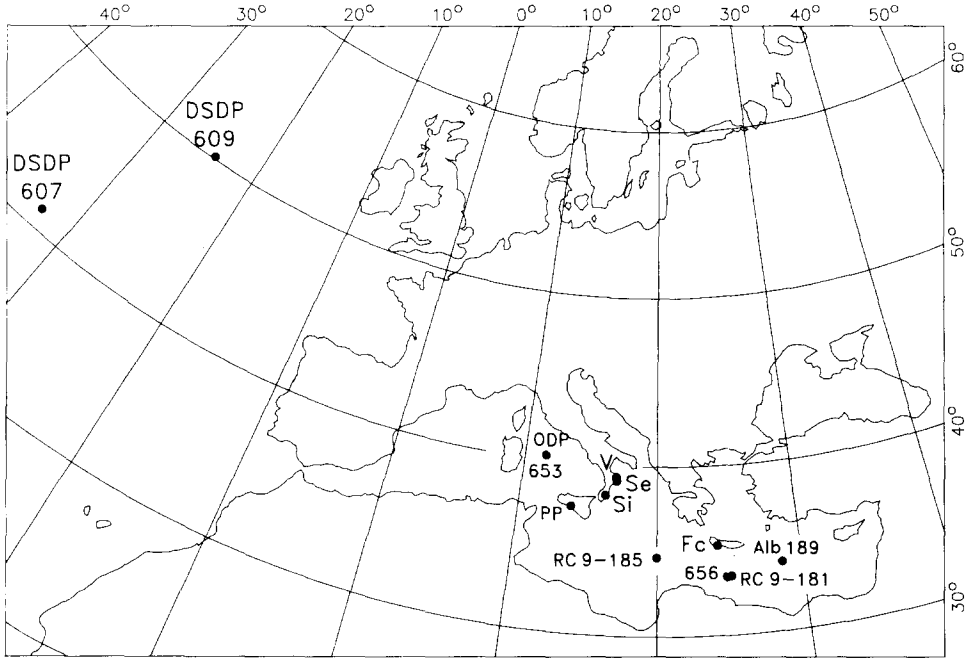

Fig. 1. Location of land sections and deep-sea cores used in this study. *PP* = Punta Piccola; *Se* = Semaforo; *Si* = Singa; *V* = Vrica; *Fc* = Francocastello.

boundaries which, except for the bottom of the Olduvai, fall within the uncertainty range of the radiometric dating [2,3,13]. Johnson [14] and Shackleton [15], on the other hand, reported ages for the Brunhes/Matuyama and Jaramillo boundaries older than those obtained by radiometric dating. Concurrent with, but independent of, the present study Shackleton et al. [1] constructed an astronomically calibrated time scale with significantly older ages for all the major reversal boundaries down to the Gauss/Matuyama boundary.

In this paper, we first establish the astronomically calibrated age of the Olduvai Subchron as recorded in the Pliocene–Pleistocene boundary stratotype section of Vrica. This is done by correlating cyclic sapropel (brownish, often laminated interbeds) patterns in the Vrica section and in the sections Semaforo, Singa, Punta Piccola and Francocastello to the astronomical solutions, using inferred phase relationships between the sapropel and orbital cycles. The resultant ages for the Olduvai, as well as for older reversal boundaries, are then compared with both conventional as well as other orbitally tuned ages for these polarity transitions.

2. The position of the Olduvai in the Pliocene–Pleistocene boundary stratotype section of Vrica

The Vrica section, in northern Calabria (Fig. 1), was formally designated as the Pliocene–Pleistocene boundary stratotype [16] after it had been intensely studied for a decade [e.g. 17–23]. The boundary was defined at the base of the homogeneous claystones which conformably overlie the sapropelic layer coded *e* in this section [16] (sapropel coding after [18], see also Fig. 2).

Initial paleomagnetic measurements on the Vrica section were carried out by Nakagawa et al. [19] who used the for this type of sediment less suitable alternating field demagnetization method [22]. Tauxe et al. [22] demonstrated that an interval of normal polarity is present in the Vrica section, which in combination with biostratigraphic evidence [23] was shown to represent the Olduvai. In addition, normal polarities were observed in the top part of the section.

Recent paleomagnetic investigations [24], however, showed that the top of the Vrica section contains reversed polarities only. The normal polarities reported earlier [22] are caused by a secondary overprint due to weathering. In ad-

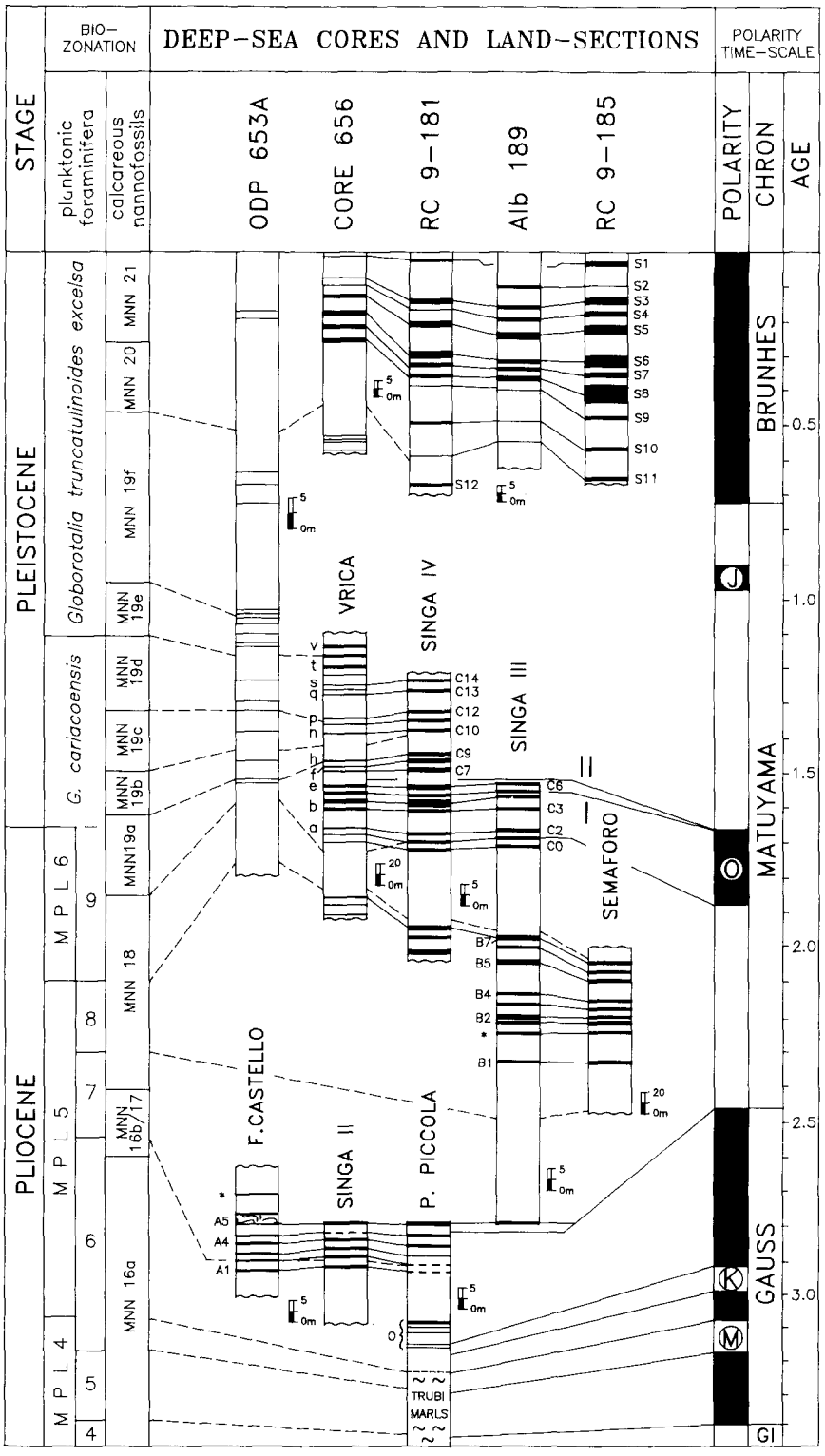
STAGE
BIO-ZONATION
planktonic foraminifera
calcareous nannofossils
DEEP-SEA CORES AND LAND-SECTIONS
ODP 653A
CORE 656
RC 9-181
Alb 189
RC 9-185
POLARITY TIME-SCALE
POLARITY
CHRON
AGE
PLEISTOCENE
PLIOCENE
Globorotalia truncatulinoides excelsa
G. cariacoensis
MNN 21
MNN 20
MNN 19f
MNN 19e
MNN 19d
MNN 19c
MNN 19b
MNN19a
MNN 18
MNN 16b/17
MNN 16a
MPL 6
MPL 5
MPL 4
9
8
7
6
5
4
VRICA
SINGA IV
SINGA III
SINGA II
F.CASTELLO
P. PICCOLA
SEMAFORO
TRUBI MARLS
S1
S2
S3
S4
S5
S6
S7
S8
S9
S10
S11
S12
C14
C13
C12
C10
C9
C7
C6
C3
C2
C0
B7
B5
B4
B2
B1
A5
A4
A1
BRUNHES
MATUYAMA
GAUSS
GI
0.5
1.0
1.5
2.0
2.5
3.0

dition, the stratigraphic position of the rather inaccurately defined lower boundary of the Olduvai is now more precisely located. The position of the top of the Olduvai, however, remains ambiguous. The new and very detailed paleomagnetic data show that reversed polarities are present in the top part of the normal polarity zone, resulting in two options for the exact position of the upper Olduvai [24]. In option I, the boundary coincides with sapropel *d* [18], implying a short normal polarity subchron slightly above the Olduvai. In option II, the boundary is located substantially higher in the succession, i.e. between sapropels *e* and *f*, and implies that an interval of reversed polarity is present in the upper part of the Olduvai. As a consequence, the Pliocene–Pleistocene boundary defined on top of the sapropelic marker bed *e* is positioned either within or slightly above the Olduvai [24].

3. Tuning the sapropels to the astronomical solutions

In the Vrica section, a total of 21 sapropelic layers have been distinguished (Fig. 2). In addition, sapropels are not only found in the Vrica section, but they occur frequently and are widespread in marine depositional sequences of the Mediterranean Neogene and Quaternary [e.g. 25,26]. Generally, they are not distributed evenly throughout the stratigraphic record but occur in distinct clusters on various scales: large-scale clusters usually comprise a number (2 to 3) of small-scale clusters which in turn contain 2 to 4 individual sapropels. The resulting patterns are complex and have been interpreted as superimposed sedimentary cycles connected with the Earth's orbital cycles, more precisely with those of precession (individual sapropels) and eccentricity (sapropel clusters) [26]. The reflection of the obliquity cycle is seemingly absent in the sedimentary record, which has been related to the relatively low (paleo-)latitudinal position of the Mediterranean [26].

In order to tune the sapropel sequence of the Vrica section to the astronomical solutions, it is necessary to determine the phase relationships between the sedimentary and orbital cycles. These phase relationships can be established by correlating the most recently deposited sapropels of late Pleistocene age in the Mediterranean to the astronomical solutions, using oxygen isotope stage boundaries for age calibration (Fig. 3). This correlation shows that individual sapropels correlate to minimum peak values of the precession index and that small- and large-scale sapropel clusters correlate to eccentricity maxima connected with the 100 and 400 ka eccentricity cycles respectively.

On the basis of these phase relationships, progressively older sapropel-bearing sequences can then be calibrated to the astronomical records by extending the tuning until the Vrica sequence is reached. However, at present this procedure is not possible due to the lack of a coherent and continuous record of middle Pleistocene sapropels, both from land sections and from deep-sea cores (Fig. 2). Although this missing interval has recently been recovered at ODP Site 653, it did not yield a sufficiently detailed sapropel record (see Fig. 2). Considering the location of this site (Tyrrhenian Sea), this is not surprising because sapropels are more frequent and widespread in the eastern Mediterranean [e.g. 27]. Unfortunately, results of deep-sea drilling in the eastern basin have also been unsuccessful because of serious coring disturbance and the sometimes poor core recovery [27,28].

Fig. 2. Review of the most relevant sapropel-bearing sequences of late Pliocene–Pleistocene age in land-based sections and deep-sea cores of the Mediterranean. Lithostratigraphy of deep-sea cores is based on Cita et al. [48], Murat and Got [49] and the Shipboard Scientific Party of ODP Leg 107 [50]. Lithostratigraphy of the land sections from Hilgen [26,31], Verhallen [29], Zachariasse et al. [33,51] and Zijderveld et al. [24]. Sapropel coding after Ryan [25] for the late Pleistocene and Selli et al. [18], Verhallen [29] and Zijderveld et al. [24] for the late Pliocene–early Pleistocene. Biozonations used are those of Cita [52] and Spaak [53] for the planktonic foraminifera and Raffi and Rio [54] for the calcareous nannofossils. Biostratigraphic data are taken from Backman et al. [23], Zijderveld et al. [24], Driever [30], Zachariasse et al. [33,51] and Glaçon et al. [55]. Also shown is the calibration to the Geomagnetic Polarity Time Scale (the conventional scale of Berggren et al. [8]) based on first-order magnetostratigraphic records (Punta Piccola section—Zachariasse et al. [33,51]; Semaforo section—Tauxe et al. [22]; Singa and Vrica sections—Zijderveld et al. [24]). Solid lines mark lithostratigraphic and magnetostratigraphic correlations, dashed lines biostratigraphic correlations.

Below this hiatus in the sapropel record, a coherent and distinctly cyclic sapropel pattern emerges again in late Pliocene–early Pleistocene sequences exposed onland. In these land sections, four successive large-scale clusters of sapropels are distinguished, separated by relatively thick intervals of homogeneous sediments. In stratigraphic order, these clusters have been coded informally as *O*, *A*, *B* and *C* ([29,30]; see Fig. 2). The Vrica section contains the uppermost sapropels of the *B*-cluster and the *C*-cluster [31]. Both in the Vrica and the Singa sections (located in nearby southern Calabria, see Fig. 1), the *C*-cluster contains a very conspicious small-scale cluster. This key-cluster contains four sapropels which are extraordinarily thick.

From the established phase relationships between the late Pleistocene sapropels and the orbital cycles (Fig. 3), it can be inferred that this prominent key-cluster corresponds not only to a 100 ka eccentricity maximum, but also to a maximum of the 400 ka eccentricity cycle, because it contains more and thicker sapropels than the adjacent small-scale clusters. In the time interval considered, 400 ka eccentricity maxima occur at 1.4 and 1.8 Ma in the astronomical solutions [32]. However, these ages do not correspond to the conventional (radiometric) age of 1.67 Ma for the top of

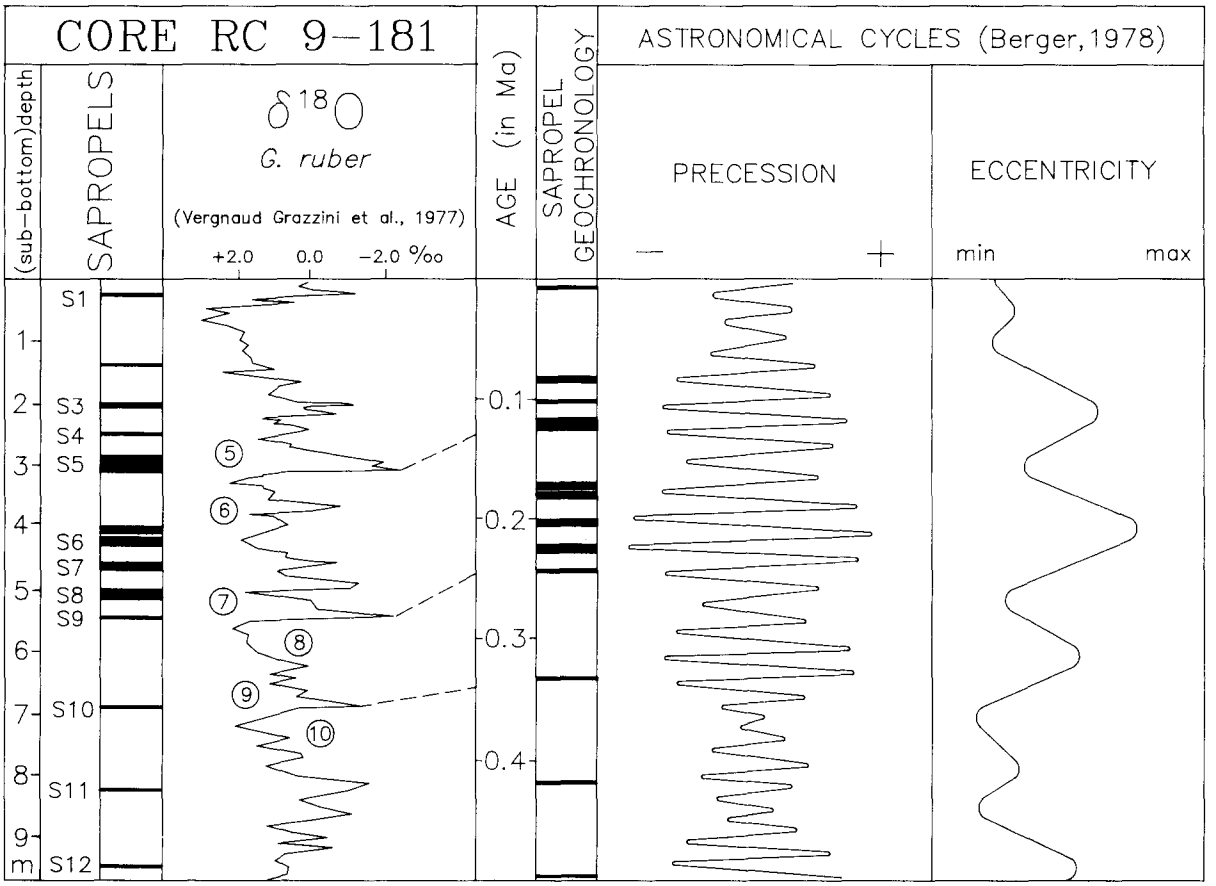

Fig. 3. Determination of phase relationships between sapropel cycles and the orbital cycles of precession and eccentricity based on the correlation of the upper Pleistocene sapropel sequence of standard core RC 9-181 in the eastern Mediterranean to the astronomical solutions. Sapropel chronology has been established according to a procedure outlined by Rossignol-Strick [46] using oxygen isotope stage boundaries 6.0, 8.0 and 10.0 dated at 128, 245 and 339 ka [9] for age calibration. The oxygen isotope record is based on Vergnaud-Grazzini et al. [47]. The astronomical records are based on the old solution of Berger [34] which is considered more accurate than the new solution for the last 1 Ma (Berger, pers. commun.)

the Olduvai [6], located either within (option I) or nearly on top (option II) of this key-cluster. The correlations of the sapropels in the lower parts of the Vrica and Singa IV sections according to both eccentricity maxima are presented in Fig. 4. Starting from the 1.4 Ma maximum, the tuning results in an age of 1.41 (option II) or 1.46 Ma (option I) for the top of the Olduvai and of 1.57 Ma for the bottom of the Olduvai. If we start from the 1.8 Ma maximum, the age for the top of the Olduvai arrives at 1.79 (option II) or 1.84 Ma (option I) and the age for the bottom of the Olduvai at 1.95 Ma (Fig. 4B). This correlation is preferred because the small-scale sapropel cluster which underlies the prominent key-cluster is more clearly reflected in the astronomical record if we use the 1.8 Ma maximum.

To determine more conclusively which of both correlations is correct, we must consider the older part of the late Pliocene–early Pleistocene sapropel record as well. The most remarkable feature in this older part of the record is the deviating pattern of sapropels found in the large-scale *A*-cluster (Fig. 2). This *A*-cluster contains a single small-scale sapropel cluster which in turn comprises no less than six successive individual sapropels. Note that the youngest but one sapropel of this cluster is missing in the Singa section. However, the pres-

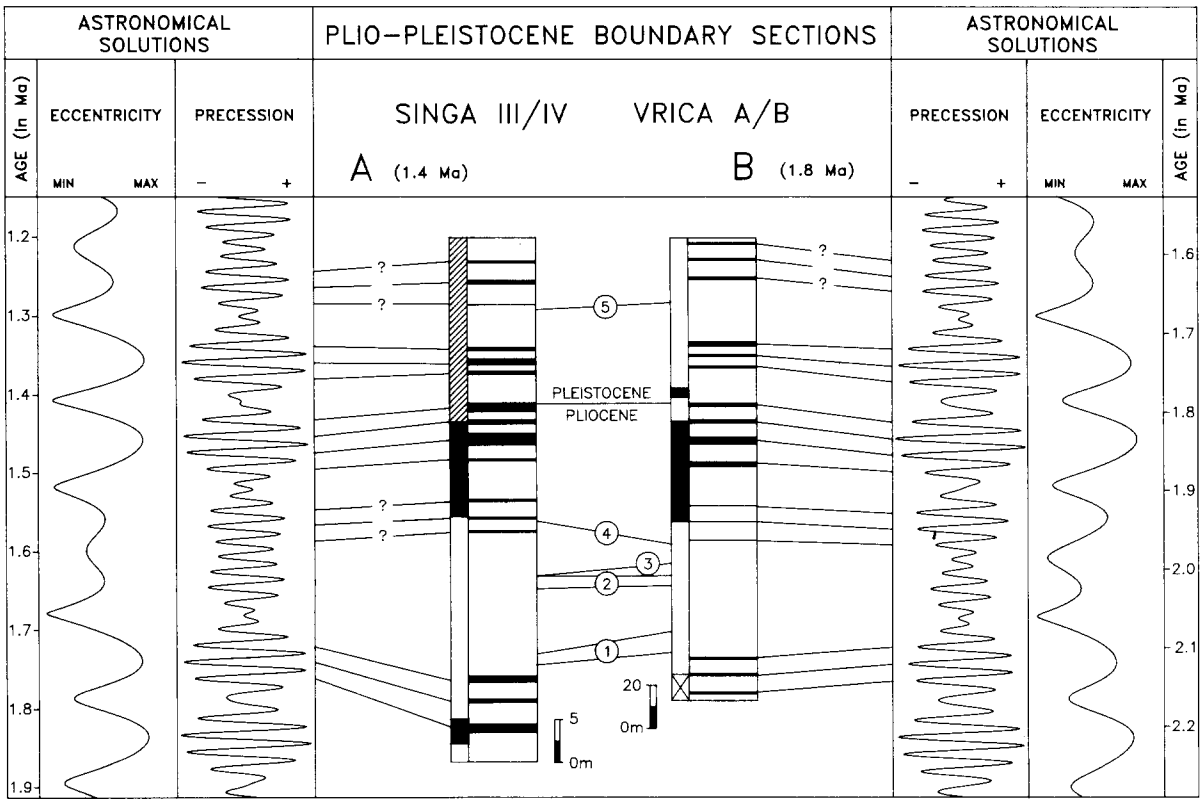

Fig. 4. The two possible alternatives for correlating the pattern of sapropels in the lower parts of the Plio-Pleistocene boundary sections of Vrica and Singa IV to the new astronomical solutions for precession and eccentricity [35] based on the established phase relationships between sapropel and orbital cycles. (A) The distinct small-scale key-cluster of four sapropels (*b–e* according to the coding of [18]; C3–C6 after [29]; see also Fig. 2) correlates with the maximum in eccentricity of the 400 ka eccentricity cycle dated around 1.4 Ma. (B) This key-cluster correlates with the successive older maximum of the 400 ka cycle of eccentricity dated around 1.8 Ma. Lithostratigraphy, biostratigraphy and magnetostratigraphy after [24,29,30]. Biostratigraphic correlations shown: *1* = *G. inflata* influx; *2* = *G. truncatulinoides* FOD and influx; *3* = *G. inflata* reapearance; *4* = *D. brouweri* LOD; *5* = *C. macintyrei* FOD. Hatching in magnetostratigraphic records denotes inconclusive paleomagnetic results or lack of data [see 24]. Astronomical records are based on the new solutions of Berger and Loutre [32; version BER – 90]. The original data by Berger and Loutre [32] cannot be reproduced without their permission.

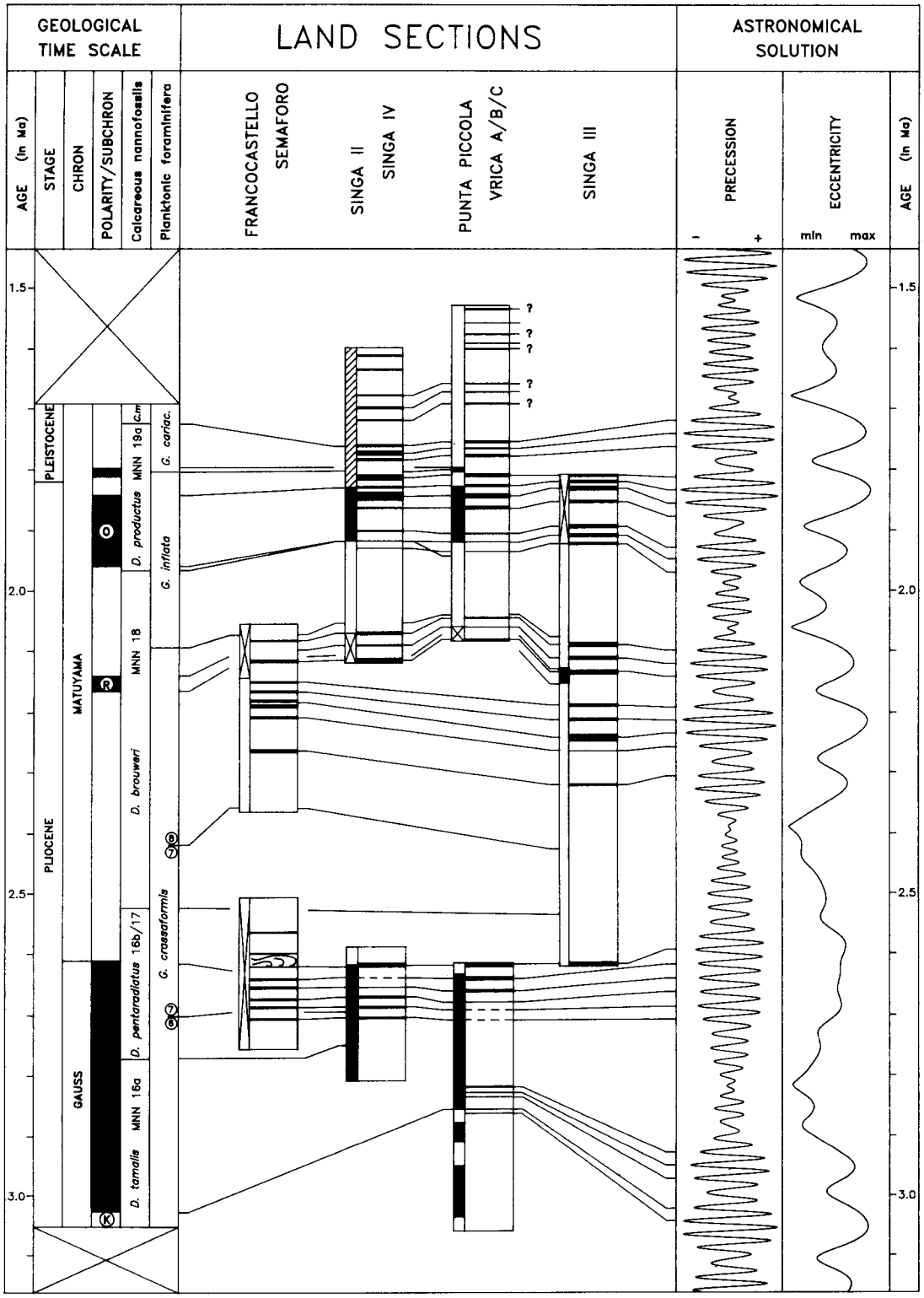

Fig. 5. Correlation of upper Pliocene–lower Pleistocene sapropel sequences to the new astronomical solutions for precession and eccentricity [32] using corresponding aberrations in the pattern of sapropels (the *A*-cluster) and the precession record for calibration. The original data by Berger and Loutre [32] cannot be reproduced without their permission. See further explanation in Fig. 2.

ence of pyritic lumps and framboids at a time-equivalent level indicates that lowered bottom-water oxygen conditions, which are responsible for the deposition of sapropels, also persisted at Monte Singa at that time [33]. At Punta Piccola, the two lowermost beds of this cluster do not contain true sapropelic sediments but merely consist of dark-coloured marly clays. The Francocastello section on Crete, on the other hand, reveals an additional (seventh) sapropel. Close inspection of the astronomical solutions reveals a remarkably similar deviation in the record of the precession index connected with the 400 ka eccentricity maximum at 2.60 Ma. In this interval, the amplitude variations of the precession index lack the usual pronounced modulation by the 100 ka eccentricity cycle, resulting in 6–7 successive, high-amplitude excursions of the precession index to negative values. The six sapropels of the *A*-cluster can now be calibrated to the astronomical record in such a way that the most prominently developed sapropels in the Singa section (A2 and A5; see also [33]) correlate with the most negative excursions of the precession index (Fig. 5). It is emphasized that the use of the new astronomical solutions of Berger and Loutre [32] is of decisive importance here. The new calculations start to deviate significantly from the old, less accurate solutions of Berger [34] at 1.5 Ma. The aberrant pattern in the precession record at 2.6 Ma is crucial to the astronomical calibration of our sapropels and it is not found in the old solution. Instead, an essentially similar deviation was observed before at 1.85 Ma.

Based on the calibration to the new solution, the remaining part of the sapropel record can be correlated straightforwardly to the astronomical record (Fig. 5). This correlation results in ages of 1.95 ($\pm$0.01) Ma for the bottom of the Olduvai, 1.84 (option I) or 1.79 Ma (option II) for the top of the Olduvai and 1.81 Ma for the Pliocene–Pleistocene boundary. It confirms that the small-scale key-cluster in the large-scale *C*-cluster indeed correlates with the 400 ka eccentricity maximum at 1.8 Ma. In addition, ages are obtained for the Reunion (2.14–2.15), the Gauss/Matuyama (2.59/2.62) and the top of the Kaena (3.02 $\pm$ 0.01), because detailed magnetostratigraphic records are presently available for the majority of these land sections (Fig. 5).

Nevertheless, some discrepancies remain, the most important of which is the correlation of the sapropels in the upper part of the Vrica section to the astronomical record. This correlation is severely hampered for several reasons. Firstly, pre-

TABLE 1

Old coding and new precession-related MPRS coding for sapropels in the Mediterranean. *1* = after Ryan [25]; *2* = after Selli et al. [18]; *3* = after Verhallen [29]. MPRS coding and lagged age using the correlative peak of the precession index as numbered from the Recent. Asterisk denotes unnamed or unnumbered sapropel

1	2	MPRS-Coding	age	lagged age	2	3	MPRS-Coding	age	lagged age	3	MPRS-Coding	age	lagged age
S1	-	2	0.012	0.008	r	-	?	-	-	B5	208	2.141	2.137
S2	-	6	0.060	0.056	q	C13	?	-	-	B4	212	2.191	2.187
S3	-	8	0.083	0.079	p	C12	?	-	-	B3	214	2.213	2.209
S4	-	10	0.106	0.102	o	C11	?	-	-	B2	216	2.235	2.231
S5	-	12	0.127	0.123	n	C10	?	-	-	*	218	2.257	2.253
S6	-	16	0.176	0.172	h	C9	168	1.719	1.715	B1	222	2.306	2.302
S7	-	18	0.198	0.194	f	C8	170	1.741	1.737	A5	250	2.593	2.589
S8	-	20	0.220	0.216	*	C7	172	1.762	1.758	*	252	2.616	2.612
S9	-	22	0.242	0.238	e	C6	176	1.812	1.808	A4	254	2.639	2.635
S10	-	30?	0.335	0.331	d	C5	178	1.834	1.830	A3'	256	2.663	2.659
S11	-	38?	0.409	0.405	c	C4	180	1.855	1.851	A2	258	2.686	2.682
S12	-	46?	0.485	0.481	b	C3	182	1.877	1.873	A1	260	2.708	2.704
-	v	?	-	-	a	C2	186	1.928	1.924	O*	280	2.928	2.924
-	u	?	-	-	-	C1	188	1.949	1.945	O*	282	2.950	2.946
-	t	?	-	-	-	C0	190	1.969	1.965	O*	284	2.972	2.968
-	*	?	-	-	-	B7	204	2.098	2.094	O*	288	3.021	3.017
-	s	?	-	-	-	B6	206	2.120	2.116	O*	290	3.042	3.038

liminary attempts to correlate the frequency distribution of sinistrally coiled neogloboquadrinids to the northern Atlantic DSDP Site 607 suggest that an hiatus is present in the top part of the Vrica section. Secondly, the characteristic cyclicity in the sapropel pattern—related to precession and eccentricity—is probably distorted in this particular interval by the following factors:

(1) The additional influence of obliquity on the distribution of the sapropels.

(2) the steady increase in the number of sapropels per large-scale cluster. This trend, which may be related to a gradual lowering of some threshold value for sapropel formation, eventually results in the disappearance of the distinct, eccentricity-related pattern in the distribution of the sapropels.

(3) Changes in sediment accumulation rate.

Current research is focussed on the solution of these problems by combining the complex sapropel pattern with a very detailed record of the frequency distribution of sinistral neogloboquadrinids. This record contains additional information on the influence of the obliquity cycle and will be reported on in a forthcoming paper. These forthcoming results will most probably not affect the calibration of the older sapropels to the astronomical record.

It is important to note that our present solution differs markedly from an earlier attempt to correlate the sapropels in the Vrica and Semaforo sections to summer insolation curves for this latitude [35]. This attempt was severely hindered by the assumption that a stratigraphic gap is present between both sections, whereas they actually proved to contain a considerable overlap [31]. Moreover, the insolation curve used by Combourieu-Nebout [35] was based on astronomical solutions which presently are considered to be less accurate for this interval of time [32].

4. A new integrated Mediterranean sapropel codation

In Table 1, we formalize our sapropel correlation to the astronomical record by introducing new coding for sapropels in the Mediterranean Pliocene–Pleistocene. In existing coding, sapropels are continuously numbered [18,25,29]. Our new Mediterranean Precession Related Sapropel (MPRS) coding is based on coding sapropels after the correlative peak of the precession index as numbered from the Recent. This MPRS coding has the distinct advantage that newly found sapropels can always be incorporated. More importantly, all coded sapropels can be dated with an accuracy of 1 ka by reference to the corresponding peak in the precession record (Table 1). For a truely accurate dating of the sapropels, a time lag of 4 ka between orbital forcing and maximum climate response and sapropel deposition must be taken into account. This time lag is based on the age of 9–6 ka for the youngest sapropel in the eastern Mediterranean (S1; [36,37]) as compared with the age of 11.5 ka for the correlative negative peak of the precession index. A time lag of 4 ka agrees well with other time lags inferred for the climate response to orbital forcing by precession [38–40].

5. Discussion

The correlation of sapropels to the astronomical solutions results in ages for the top of the Olduvai (1.79 or 1.84 Ma), the bottom of the Olduvai (1.95 ± 0.01), the Reunion (2.14–2.15), the Gauss/Matuyama (2.59/2.62) and the top of the Kaena (3.02 ± 0.01). These ages deviate considerably from conventional ages which are either based on K/Ar radiometric dating only [6] or on linear interpolation between radiometrically dated calibration points in marine anomaly sequences [e.g. 8]. In addition, they also differ from ages which have been established previously by orbital tuning procedures and which have essentially confirmed the radiometric datings [2,3,13] (see Table 2). It is easily shown that no apparent relationships exist between our sapropel pattern and the precession record if we use either the conventional polarity time scale of Berggren et al. [8] or the orbitally tuned polarity time scale of Ruddiman and Raymo [2,3] (Fig. 6).

On the other hand, the ages reported here are almost identical to those obtained recently by Shackleton et al. ([1]; table 2). Both time scales have been established using totally independent data-sets and basically the same orbital tuning method. The time scale of Shackleton et al. [1] was contructed on the basis of the high-resolution oxygen isotope record from ODP Site 677, located in the low-latitude eastern Pacific, whereas we

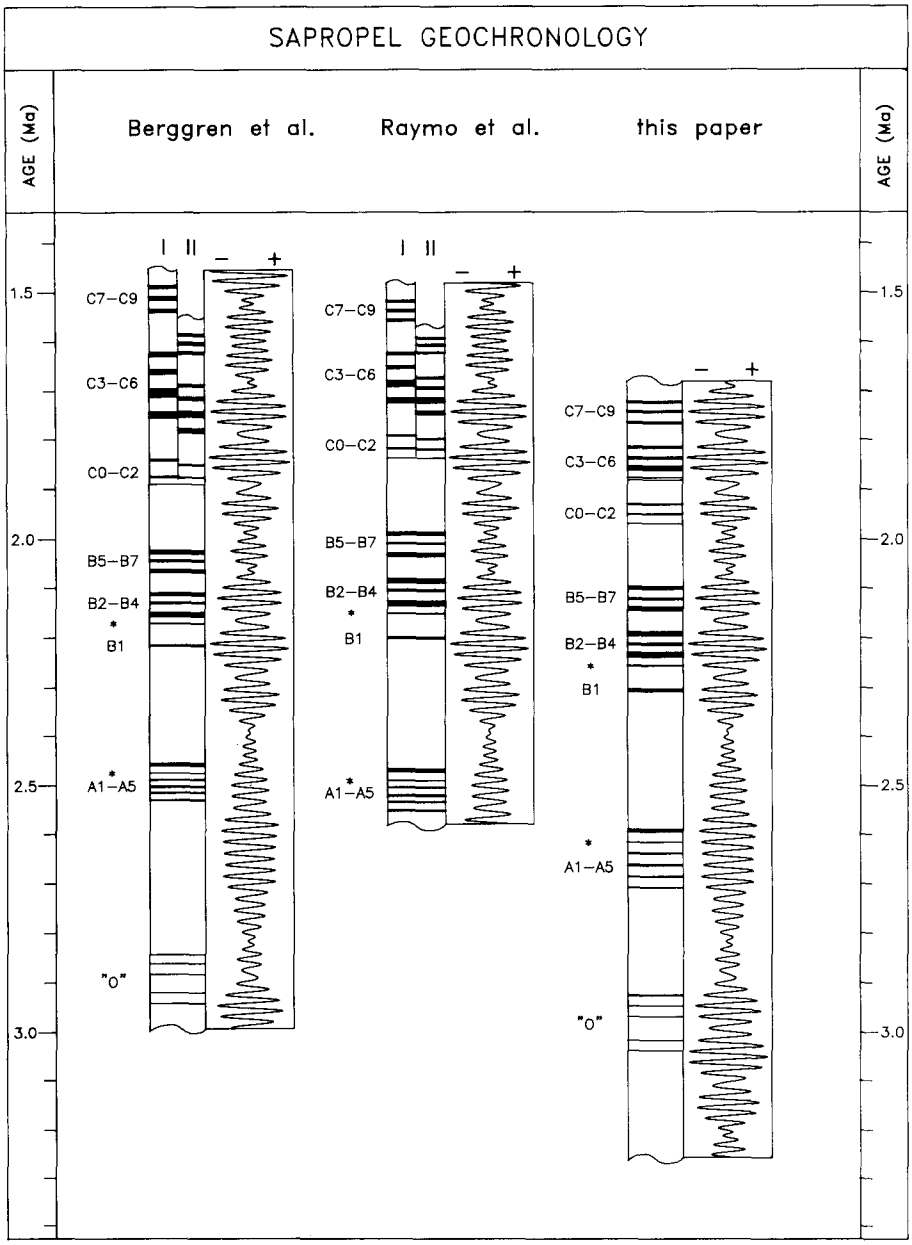

Fig. 6. Sapropel chronologies for the late Pliocene–early Pleistocene according to the different time scales. Our chronology is based on the correlation of sapropels to the astronomical solutions shown in Fig. 5. In the case of the polarity time scales of Berggren et al. [8] and Raymo et al. [3], the sapropel chronology is based on linear inter- or extrapolation of sediment accumulation rates using magnetostratigraphic datum planes for age calibration. The Singa section was employed for the interval between the base of the *A*-cluster to the base of the *C*-cluster. From the base of the *C*-cluster onward, we used the Vrica section instead; note that for the time scales of Berggren et al. [8] and Raymo et al. [3] two alternative sapropel chronologies are shown for this interval based on the two different options (I and II) for the position of the top of the Olduvai. The Punta Piccola section was used for the lowermost sapropels (*O*-cluster). The original data by Berger and Loutre [32] cannot be reproduced without their permission.

used the sapropel record in the Mediterranean. However, our tuning procedure strongly resembles the procedure followed by Shackleton et al. [1] in employing the precession rather than the obliquity component in climatic proxy records. The latter has been used in other attempts to establish an

TABLE 2

Ages for polarity reversals according to the different time scales. *M&D* = Mankinen and Dalrymple [6]; *R&R* = Ruddiman et al. [2] and Raymo et al. [3]

reversal boundary	M&D, 1979	Berggren et al., 1985	R&R, 1989	Shackleton et al., in press	this paper
Brunhes/Matuyama	0.73	0.73	0.73	0.78	-
Olduvai top	1.67	1.66	1.65	1.77	1.79 (II)
	-	-	-	-	1.84 (I)
Olduvai bottom	1.87	1.88	1.82/1.83	1.95	1.95
Reunion 1 top	2.01	-	1.98/2.00	-	2.14
Reunion 1 bottom	2.04	-	2.02	-	2.15
Reunion 2 top	2.12	-	-	-	-
Reunion 2 bottom	2.14	-	-	-	-
Gauss/Matuyama	2.48	2.47	2.48/2.49	2.60	2.59/2.62
top Kaena	2.92	2.92	-	-	3.02

astronomically calibrated time scale for the late Pliocene to early Pleistocene [2,3,13], but is considered less suitable because of the regular character of the obliquity cycle. The precession signal, on the other hand, displays a far more distinctive pattern due to its modulation by eccentricity. A difference in the procedures followed is that Shackleton et al. [1] employed the Recent as a fixed calibration point, while we established our time scale independently of the Recent by correlating similar deviating patterns in the geological and astronomical records.

5.1. Discrepancies with other astronomically calibrated time scales

A comparison of the astronomically calibrated polarity time scale of Ruddiman et al. [2] and Raymo et al. [3] and ours shows that the age discrepancy for the reversal boundaries is remarkably constant, i.e. 130 ka. An exception is the older age for the top of the Olduvai in our time scale (option I in Table 2) in which case the discrepancy is even larger. This constant discrepancy, and the resulting younger ages of the sapropels according to their time scale (Fig. 6), cannot be explained by a lag effect of approximately 100 ka connected with the 400 ka eccentricity cycle because the expression of eccentricity in our sapropel record merely reflects the modulation of precession by eccentricity (see also the remarks on p. 432 in [3]). Also, the correlation of late Pleistocene sapropels to the astronomical record (Fig. 3) does not reveal any indication of the existence of such a time lag. It is therefore anticipated that the origin of this discrepancy must be found in the interval younger than the Olduvai. According to our time scale, the age of the top of the Olduvai is either 1.84 (option I) or 1.79 Ma (option II), which in both cases departs markedly from the age of 1.65 Ma obtained by Ruddiman et al. [2]. As a consequence, the duration of the interval between the Brunhes/Matuyama and the top of the Olduvai differs from 0.92 Ma [2] to 1.06 or even 1.11 Ma (our options II and I) if we also use an age of 0.73 Ma for the Brunhes/Matuyama boundary. In order to explain this discrepancy, we have re-examined the records of Site 607 on which Ruddiman et al. [2] and Raymo et al. [3] based their time scale.

Ruddiman et al. [2] proceeded from an age of 0.73 Ma for the Brunhes/Matuyama boundary to establish an orbitally tuned (polarity) time scale for the older part of the Pleistocene by extrapolating the 41 ka quasi-period of obliquity as the periodicity of distinct cyclic changes in their $\delta^{18}O$ and $CaCO_3$ records. This approach, however, depends critically on neither skipping cycles nor adding extra ones [2, p. 359]. It is not surprising that, if their obliquity-tuned time scale is used for calibration (according to this tuning procedure, the cycles in the original records are either slightly stretched or compressed to fit the 41 ka period), spectral analysis applied on the records from Site 607 yields a single dominant peak corresponding exactly to a periodicity of 41 ka (fig. 13 in [2]). If, on the other hand, the conventional magnetic polarity time scale is used, the resulting spectrum shows that this peak has shifted to slightly higher frequencies (fig. 4 in [41]). We also applied spec-

tral analysis to the $\delta^{18}O$ and $CaCO_3$ records of Site 607, using the conventional ages of 0.73 and 1.66 Ma for the Brunhes/Matuama and the top of the Olduvai [8]. For our purpose, we used a spectral analysis program in which the Fourier transform is applied to the autocorrelation function

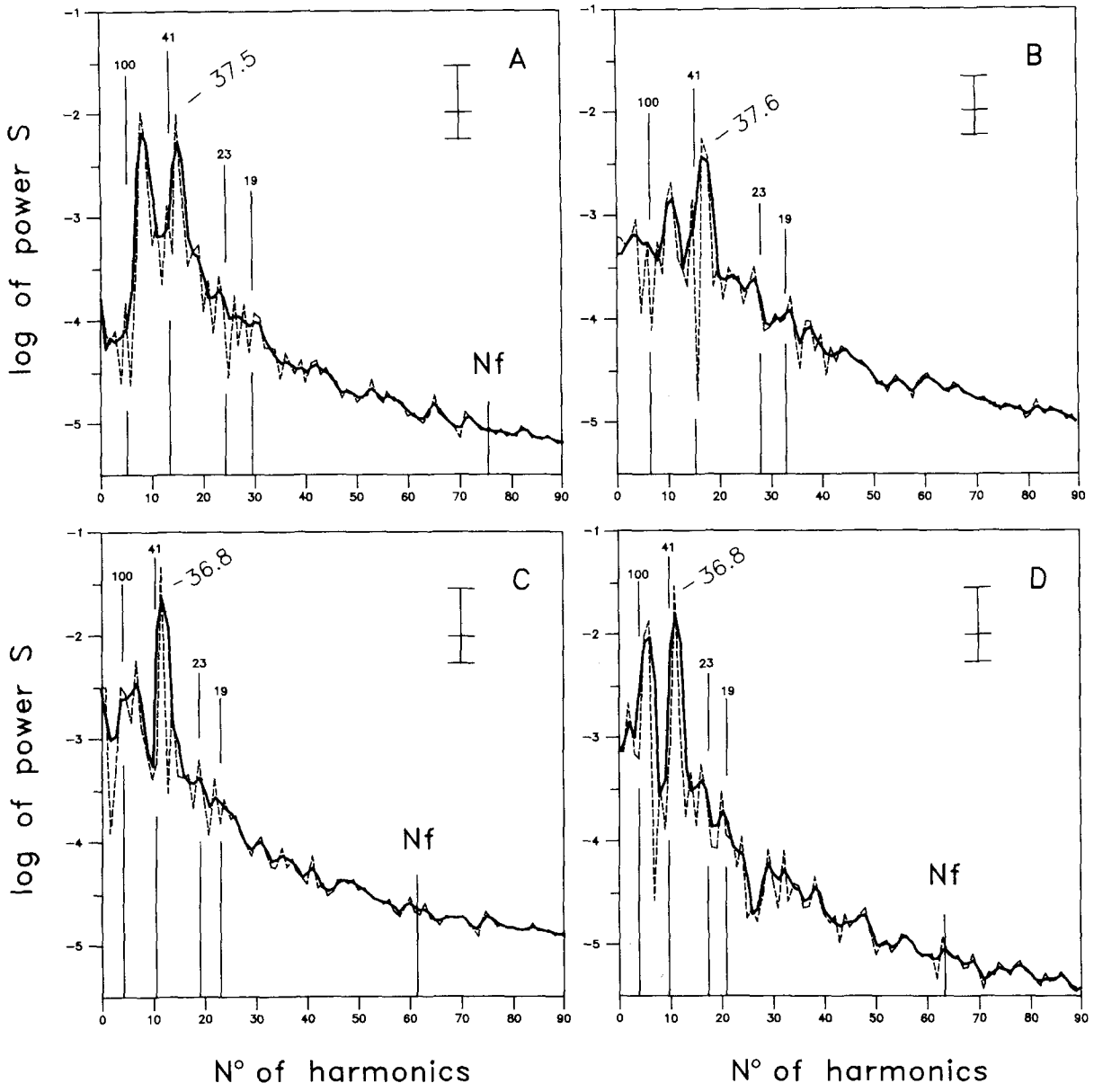

Fig. 7. Representative spectra based on the $\delta^{18}O$ (A and C) and $CaCO_3$ (B and D) records from DSDP Site 607 as published in Ruddiman et al. [2] and Raymo et al. [3]. (A) and (B) based on the interval between the Brunhes/Matuyama and the top of the Olduvai using the conventional ages of 0.73 and 1.66 Ma of the respective reversal boundaries [8] for age calibration. (C) and (D) based on the interval between the Gauss/Matuayama and the bottom of the Olduvai using the respective conventional ages of 2.47 and 1.88 Ma for calibration. The periodicity of the dominant peak in the obliquity frequency domain is shown in ka. Also indicated are the positions of frequencies corresponding to the main quasi-periods of the orbital cycles. *Nf* = Nyquist frequency of original time series using twice the average time spacing. The 80% confidence interval is shown as a small vertical bar on the right-hand side of each spectrum.

[42] of an equally spaced time series of the original record. By slightly changing the number of lags of that part of the autocorrelation function on which the Fourier transform is employed, the exact position of the spectral peaks can be accurately determined. Figure 7A shows that the most prominent peak of the $\delta^{18}O$ spectrum has indeed shifted to a higher frequency and matches a periodicity of 37.4 ± 0.1 ka. The $CaCO_3$ spectrum is more complex and yields two separate peaks with periodicities of 34.9 ± 0.1 and 37.9 ± 0.1 ka. In addition, a less prominent and significant peak is found at a frequency corresponding to a periodicity of 43.6 ka. Nevertheless, the $CaCO_3$ spectrum too shows a strong tendency to shift to higher frequencies (Fig. 7B).

This shift in the dominant spectral peak(s) in the obliquity frequency band to a higher frequency than that of the dominant quasi-period of obliquity can be explained by assuming that the interval between the Brunhes/Matuyama and the top of the Olduvai lasted longer than suggested by the conventional ages of 0.73 and 1.66 Ma for these reversal boundaries. If we correct for this frequency shift so that the corresponding periodicity matches the main 41 ka quasi-period, the estimate of the amount of time in this interval increases from 0.93 to 1.02 Ma, an increase of 90 ka. A repetition of this procedure, using the ages of 0.73 and 1.65 Ma of Ruddiman et al. [2], results in a corresponding increase from 0.92 to 1.02 Ma. At the same time, these results imply that Ruddiman et al. [2] failed to notice at least two obliquity-related cycles in this particular interval. Close inspection of the $\delta^{18}O$ and $CaCO_3$ records from Site 607 indeed reveals that the stratigraphic distance between their glacial stages 20 and 22 and between 34 and 36 is almost twice the distance normally observed in this interval, indicating that two extra cycles are present but not distinctly manifested. The reflection of these extra cycles, however, is clearly detectable in the records of Site 609 (fig. 2 in [41]; fig. 11 in [2]). To provide further support for this alternative interpretation, we applied a Tukey band-pass filter centred at a frequency of 0.0267 cycles per year (i.e. corresponding to a periodicity of 37.4 ka as indicated by the results of our spectral analysis) to the conventional time-series of the records from Site 607. The filtered components clearly reveal the two extra obliquity-related cycles missed by Ruddiman et al. (Fig. 8A). Moreover, comparison with the actual, but lagged record of obliquity confirms that these components contain two extra cycles in this interval (Fig. 8B). Essentially the same results are obtained if we apply a band-pass filter centred at the main orbital frequency of obliquity of 0.0244 cycles per year (a periodicity of 41 ka). Consequently, the estimate of 0.92 Ma of Ruddiman et al. [2] for the duration of this interval would increase by 82 ka to 1.0 Ma. Shackleton et al. [1] independently arrived at more or less the same conclusion although they interpreted Stage 21 to contain three precession peaks rather than two obliquity peaks.

Although this re-examination of Site 607 reveals that as much as 1.02 Ma may be present between the Brunhes/Matuyama and the top of the Olduvai, this still does not agree with our estimates of 1.06 (option II) or 1.11 Ma (option I). It must be remembered, however, that our estimates depended on an age of 0.73 Ma for the Brunhes/Matuyama boundary. Following the earlier ideas of Johnson [14], Shackleton et al. [1] convincingly demonstrated that the (orbitally tuned) age of 0.73 Ma is too young and that the

Fig. 8. Time-series of the variations in $\delta^{18}O$ and $CaCO_3$ and their filtered obliquity components for the interval between the Brunhes/Matuyama and the top of the Olduvai at DSDP Site 607 using either the conventional ages of 0.73 and 1.66 Ma [8] (A) or the new astronomically calibrated ages of 0.78 [1] and 1.79 Ma (C) of these reversal boundaries. The Tukey band-pass filters were centred at frequencies of 0.0267 (dotted line in (A); bandwidth = 0.104) and 0.0244 (dashed lines in (A) and (C); bandwidth = 0.095) cycles per year. The former corresponds to a periodicity of 37.4 ka, as indicated by the results of spectral analysis (see Fig. 7), the latter to the main 41 ka quasi-period of obliquity. Arrows mark the obliquity-related cycles missed by Ruddiman et al. [2]. Note that the $\delta^{18}O$ and $CaCO_3$ records have been detrended and averaged around zero. Variations in obliquity and the corresponding frequency components of $\delta^{18}O$ and $CaCO_3$ at DSDP Site 607 for the Brunhes/Matuyama to top Olduvai interval are also shown. Frequency components taken from Fig. 8A are shown in (B) and those from Fig. 8C are shown in (D). Solid line shows 8 ka lagged versions of actual obliquity after the new astronomical solutions [32]. The original data by Berger and Loutre [32] cannot be reproduced without their permission. Note that the filtered components have been normalized to obliquity.

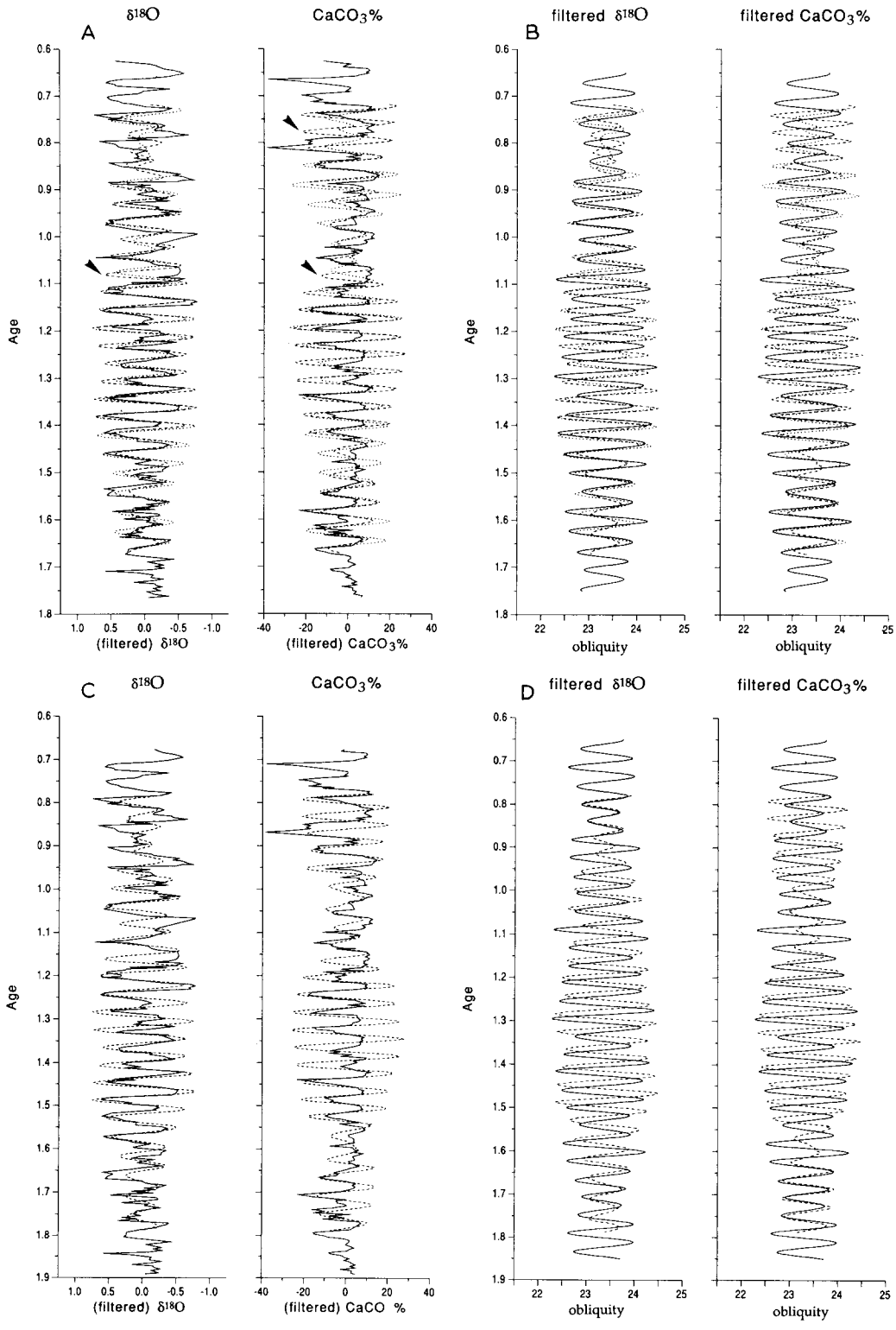
A
δ18O
CaCO3%
B
filtered δ18O
filtered CaCO3%
C
δ18O
CaCO3%
D
filtered δ18O
filtered CaCO3%
Age
(filtered) δ18O
(filtered) CaCO3%
(filtered) CaCO %
obliquity

TABLE 3

Age differences between our polarity time scale and those of Ruddiman et al. (1989) [2] and Raymo et al. (1989) [3], and Mankinen and Dalrymple (1979) [6]. These differences are also given as the percentage of their ages for the reversals. The age of 0.78 Ma* for the Brunhes/Matuyama boundary is taken from Shackleton et al. [1]

reversal boundary	our	Ruddiman & Raymo, 1989			Mankinen & Dalrymple, 1979		
	age	age	Δ	%	age	Δ	%
Brunhes/Matuyama	(0.78)*	0.73	0.05*	6.85*	0.73	0.05*	6.85*
Olduvai top	1.79	1.65	0.14	8.48	1.67	0.12 (II)	7.19
	1.84	-	0.19	11.52	-	0.17 (I)	10.18
Olduvai bottom	1.95	1.82	0.13	7.14	1.87	0.08	4.28
Reunion top	2.14	1.99	0.15	7.54	-	-	-
Reunion bottom	2.15	2.02	0.13	6.44	-	-	-
Gauss/Matuyama	2.59/2.62	2.48	0.11/0.14	5.04	2.48	0.11/0.14	5.04
Kaena top	3.02	-	-	-	2.92	0.10	3.43

actual age for the Brunhes/Matuyama is 0.78 Ma. As a consequence of this new age, the duration of the Brunhes/Matuyama to Olduvai period is reduced by 50 ka to either 1.06 (option I) or 1.01 Ma (option II). In conclusion, our estimate is now consistent with the record of Site 607 if we use the younger age of the top of the Olduvai (option II in Table 2). In option I, the Olduvai would only span 110 ka, which is definitely too short (Table 2), while according to the preferred second option, the Olduvai lasts 160 ka [24]. This agrees well with the estimate of 170 ka of Raymo et al. [3] and the 180 ka of Shackleton et al. [1]. Moreover, the resulting astronomically calibrated age of 1.79 Ma for the top of the Olduvai is close to the age estimate of 1.77 Ma of Shackleton et al. [1] for this boundary.

As a final test of our age model, a band-pass filter centred at the dominant frequency of obliquity was again applied to the records from Site 607, but this time we employed the new astronomically calibrated ages of the Brunhes/Matuyama (0.78 Ma) and the top of the Olduvai (1.79 Ma) to generate the time series. The filtered components are almost exactly in phase with actual obliquity at the age calibration points, but they are slightly out of phase in between (Fig. 8D). Very importantly, however, they do contain the same number of cycles, suggesting that slight changes in sedimentation rate are responsible for the observed out of phase relationship in between the calibration points. The near in-phase relationship observed at the top of the Olduvai further indicates that 1.79 Ma (or 1.78) is a more accurate age for this reversal boundary than the 1.77 Ma suggested by Shackleton et al. [1]. This discrepancy might be explained by the slight uncertainty concerning the exact position of this boundary with respect to the isotopic stages (see [2]). Shackleton et al. [1] listed the base of Stage 63 as the position of this reversal boundary, whereas at Site 607 it actually occurs in the top part of Stage 64 [3]. The latter position determines the near in-phase relationship between the filtered components and lagged obliquity at the top of the Olduvai in Fig. 8D.

In order to have an additional check on our ages for reversal boundaries older than the Olduvai, we have applied spectral analysis to the interval between the Gauss/Matuyama and the bottom of the Olduvai at Site 607, followed by the adjustment of consistent shifts of the dominant peak in the obliquity frequency domain with respect to the main frequency of obliquity. The resultant spectra for both the variations in $\delta^{18}O$ and $CaCO_3$% revealed a single peak in this frequency domain corresponding to a periodicity of 36.8 ± 0.1 ka, if the conventional ages of 1.88 and 2.47 Ma for the bottom of the Olduvai and the Gauss/Matuyama [8] are used (Figs. 7C and D). The correction necessary to adjust for this consistent frequency shift results in an increase of the duration of this particular interval from 0.59 to 0.66 Ma. This perfectly matches both the estimate of Raymo et al. [3], indicating that no obliquity-related cycles have been missed in this interval, as well as our estimate and that of Shackleton et al. [1] (see Table 2). It deviates,

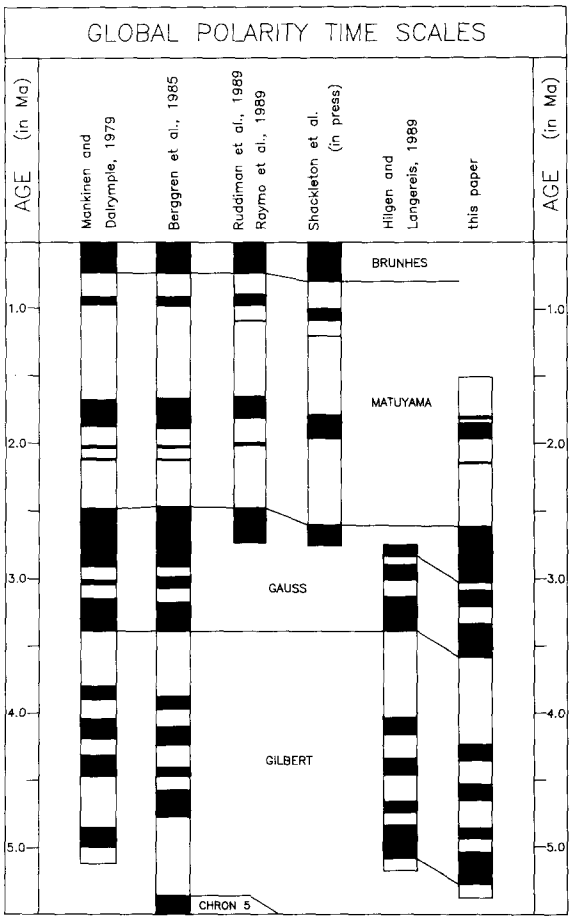

Fig. 9. Comparison of the extended astronomical time scale with other polarity time scales.

however, considerably from the duration of this interval according to the more conventional time scales [6,8].

5.2. Discrepancies between radiometric ages for polarity reversals

The discrepancies between our astronomically calibrated polarity time scale and the conventional time scales (Tables 2 and 3, Fig. 9), which for this period of time rely heavily on K/Ar radiometric dating, are more difficult to explain. Although we cannot provide a solution to this problem, a comparison between these methodologically totally different time scales shows that the discrepancy is, proportionally, fairly constant if only the radiometrically more accurately dated Brunhes/Matuyama and Gauss/Matuyama Chron boundaries are considered (5–7%; see Table 3). Possible errors in the radiometric dating method include the inaccuracy of the decay constants (note that these constants were readjusted in 1979 which resulted in an increase in the K/Ar ages by 2.66% for the period of time under consideration [43]), the imperceptible loss of radiogenic argon and the (possible) lack of sensitivity in accurately measuring low concentrations of radioactive decay gas at such young levels. It is expected that new radiometric methods, such as single crystal laser dating, will give more insight into the accuracy of the K/Ar ages and thereby in the origin of the discrepancy between the radiometric and astronomically calibrated ages for reversal boundaries.

5.3. Extension of the astronomically calibrated time scale to the Miocene/Pliocene boundary

The procedure of tuning climatic proxy records to the new astronomical solutions is a very promising tool for constructing a truely high-resolution time scale for at least the last 5–10 Ma, i.e. the period of time for which the astronomical solutions are now considered to be reliable [32]. At present, this time scale can be extended back to the Miocene/Pliocene boundary if we also take the detailed record of small-scale, precession-related $CaCO_3$ cycles in the Trubi Formation on Sicily [44] into account. For these Trubi marls, we also found a remarkably consistent shift in spectral peaks to frequencies higher than the orbital frequencies. This shift has been explained by assuming that the conventional ages assigned to reversal boundaries were not sufficiently accurate. In addition, an alternative time scale was provided for the major part of the Gilbert and Gauss Chrons by extrapolating an average quasi-period of 21.7 ka of the precession cycle [45] as the periodicity of these small-scale cycles, using the Gilbert/Gauss Chron boundary dated radiometrically at 3.40 Ma as a fixed age reference point. The thus obtained age of 2.84 Ma for the top of the Kaena, however, is significantly younger than our present age of 3.02 Ma for this boundary. By adding this difference of 180 ka to the ages assigned to reversal boundaries by Hilgen and Langereis [44], our orbitally tuned polarity time scale is extended back to the Miocene/Pliocene boundary (Fig. 8). This results in an age of 3.58 Ma for the Gilbert/Gauss boundary, which is 5.3% older than the conventional radiometric age of 3.40 Ma. This

confirms the proportional constancy of the age discrepancy between our time scale and the radiometric scale. The extension of the astronomically calibrated time scale to the Miocene/Pliocene boundary will be presented in more detail in a separate paper.

6. Conclusions

The calibration of cyclic sapropel patterns of late Pliocene to early Pleistocene age to the new astronomical solutions for precession and eccentricity [32] results in ages for the top of the Olduvai (1.79 Ma), the bottom of the Olduvai (1.95 ± 0.01), the Reunion (2.14–2.15), the Gauss/Matuyama (2.59–2.62) and the top of the Kaena (3.02 ± 0.01). The age for the Pliocene/Pleistocene boundary arrives at 1.81 Ma.

This tuning furthermore provides an excellent opportunity for introducing a Mediterranean Precession-Related Sapropel (MPRS) coding according to which sapropels in the Mediterranean Pliocene–Pleistocene are coded using the correlative peak of the precession index as numbered from the Recent. These sapropels can be dated with an accuracy of 1 ka if we consider a time lag of 4 ka between orbital forcing and maximum climate response and sapropel formation, as observed for the youngest, Holocene sapropel.

Our ages are remarkably identical to the independently established, astronomically calibrated ages of Shackleton et al. [1]. The age discrepancy of 130 ka between our new polarity time scale and that of Ruddiman et al. [2] and Raymo et al. [3] is explained by the age of 0.78 instead of 0.73 Ma for the Brunhes/Matuyama (50 ka), in combination with the finding that Ruddiman et al. [2] most probably missed two obliquity-related cycles (80 ka) in the interval between the Brunhes/Matuyama and the top of the Olduvai in the records from DSDP Site 607.

A proportionally constant age discrepancy is found between our polarity time scale and the conventional polarity time scales which depend primarily on K/Ar radiometric dating. This discrepancy of 5–7% cannot easily be explained at present and must await further research.

In order to confirm our age model, it is necessary to complete the sapropel record of the Mediterranean Pliocene–Pleistocene by the recovery of continuous and relatively undisturbed marine sequences from the eastern Mediterranean, preferably by hydraulic piston coring of multiple holes. Continued work in the Mediterranean is especially relevant because the Mediterranean is a marginal sea, which is particularly sensitive to the climatic effect of precession due to its low latitudinal position, its basin configuration and the related hydrological conditions. Due to the modulation by eccentricity, the precession signal is far more distinctive than that of the more regular obliquity cycle. We therefore consider the precession-dominated sedimentary record of the Mediterranean more suitable for the construction of an astronomically calibrated time scale than the isotope records from DSDP Site 607 or even ODP Site 677, which primarily reflect the dominant control of the obliquity cycle on global ice volume.

Finally, our astronomically calibrated time scale can be extended back to the Miocene/Pliocene boundary by incorporating the time scale of Hilgen and Langereis [44] for the major part of the Gilbert and Gauss Chrons and adding the difference of 180 ka for the age of the top of the Kaena to the ages assigned to the older reversal boundaries in Hilgen and Langereis' time scale.

Acknowledgements

T. van Hinte skillfully made the drawings. A. Berger and M.F. Loutre kindly provided their new astronomical records. The stimulating discussions with A. Berger, W.A. Berggren, P. de Boer, C.G. Langereis, L. Lourens, M.F. Loutre, N.J. Shackleton and W.J. Zachariasse are gratefully acknowledged and they led to considerable improvement of the manuscript. J. Imbrie and an anonymous reviewer are thanked for their reviews. This study was partly funded by the Netherlands Organization for Scientific Research (NWO).

References

1 N.J. Shackleton, A. Berger and W.R. Peltier, An alternative astronomical calibration of the Lower Pleistocene time scale based on ODP Site 677, Trans. R. Soc. Edinb., 81, 251–261, 1990.

2 W.F Ruddiman, M.E. Raymo, D.G. Martinson, B.M. Clement and J. Backman, Pleistocene evolution: Northern hemisphere ice sheets and North Atlantic Ocean, Paleoceanography 4, 353–412, 1989.

3 M.E. Raymo, W.F. Ruddiman, J. Backman, B.M. Clement and D.G. Martinson, Late Pliocene variation in northern Hemisphere ice sheets and North Atlantic deep water circulation, Paleoceanography 4, 413–446, 1989.
4 C.S. Gromme and R.L. Hay, Magnetization of basalt bed I, Olduvai Gorge, Tanganyika, Nature 200, 560–561, 1963.
5 C.S. Gromme and R.L. Hay, Geomagnetic polarity epochs: Age and duration of the Olduvai normal polarity event, Earth Planet. Sci. Lett. 10, 179–185, 1971.
6 E.A. Mankinen and G.B. Dalrymple, Revised geomagnetic polarity time scale for the interval 0–5 m.y. B.P., J. Geophys. Res. 84, 615–626, 1979.
7 W.B. Harland, A.V. Cox, P.G. Llewellyn, A.G. Smith and R. Walters, A geological tIme Scale, Cambridge University Press, Cambridge, 127 pp. 1982.
8 W.A. Berggren, D.V. Kent, J.J. Flynn and J.A. Van Couvering, Cenozoic geochronology, Geol. Soc. Am. Bull., 96, 1407–1418, 1985.
9 J. Imbrie, J.D. Hays, D.G. Martinson, A. McIntyre, A.C. Mix, J.J. Morley, N.G. Pisias, W.L. Prell and N.J. Shackleton, The orbital theory of Pleistocene climate: Support from a revised chronology of the marine $\delta^{18}O$ record, in: Milankovitch and Climate, NATO ASI Ser. C, 126, A.L. Berger et al., eds., Reidel, Dordrecht, pp. 269–305, 1984.
10 J.D. Hays, J. Imbrie and N.J. Shackleton, Variations in the earth's orbit: Pacemaker of the ice ages, Science 194, 1121–1132, 1976.
11 J.J. Morley and J.D. Hays, Towards a high-resolution, global, deep-sea chronology for the last 750,000 years, Earth Planet. Sci. Lett. 53, 279–295.
12 D.G. Martinson, N.G. Pisias, J.D. Hays, J. Imbrie, T.C. Moore and N.J. Shackleton, Age dating and the orbital theory of the ice ages: Development of a high-resolution 0 to 300,000-year chronostratigraphy, Quat. Res. 27, 1–29, 1987.
13 N.G. Pisias and T.C. Moore, The evolution of Pleistocene climate: A time series approach, Earth Planet. Sci. Lett. 52, 450–458, 1981.
14 R.G. Johnson, Brunhes–Matuyama dated at 790,000 yr B.P. by marine astronomical correlations, Quat. Res. 17, 135–147, 1982.
15 N.J. Shackleton, A case for revising the astronomical calibration for the Brunhes–Matuyama and Jaramillo boundaries, Terra Abstr. 1, 185, 1989.
16 E. Aquirre and G. Pasini, The Pliocene–Pleistocene boundary, Episodes 8, 116–120, 1985.
17 G. Pasini, R. Selli, R. Tampieri, M.L. Colalonga, S. d'Onofrio, A.M. Borsetti and F. Cati, The Vrica section, in: The Neogene–Quaternary Boundary, II Symp. Bologna–Crotone, Excursion Guide-book, R. Selli, ed., pp. 62–72, 1975.
18 R. Selli, C.A. Accorsi, M. Bandini Mazzanti, D. Bertolani Marchetti, G. Bigazzi, F.P. Bonnadonna, A.M. Borsetti, F. Cati, M.-L. Colalonga, S. d'Onofrio, W. Landini, E. Menesini, R. Mezzeti, G. Pasini, G. Savelli and R. Tampieri, The Vrica section (Calabria). A potential Neogene–Quaternary boundary stratotype, G. Geol. 41, 181–204, 1977.
19 H. Nakagawa, N. Niitsuma, T. Takayama, S. Tokunaga, H. Kitazato and I. Koizumi, Preliminary results of magneto- and biostratigraphy of the Vrica section (Calabria, southern Italy), Proc. 2nd Symp. Neogene/Quaternary Boundary (U.S.S.R., 1977), pp. 145–156, 1980.
20 H. Nakagawa, Neogene/Quaternary boundary and correlation of Vrica section, Proc. Neogene/Quaternary Boundary Field Conference (India, 1979), pp. 107–111, 1981.
21 J.D. Obradovitch, C.W. Naeser, G.A. Izett, G. Pasini and G. Bigazzi, Age constraints on the proposed Plio-Pleistocene boundary stratotype at Vrica, Italy, Nature 298, 55–59, 1982.
22 L. Tauxe, N.D. Opdyke, G. Pasini and C. Elmi, Age of the Plio-Pleistocene boundary in the Vrica section, southern Italy, Nature 304, 125–129, 1983.
23 J. Backman, N.J. Shackleton and L. Tauxe, Quantitative nannofossil correlation to open ocean deep-sea sections from Plio-Pleistocene boundary at Vrica, Italy, Nature 304, 156–158, 1983.
24 J.D.A. Zijderveld, F.J. Hilgen, C.G. Langereis, P.J.J.M. Verhallen and W.J. Zachariasse, Integrated magnetostratigraphy and biostratigraphy of the Upper Pliocene–Lower Pleistocene from the Monte Singa and Crotone areas in Calabria (Italy), Earth Planet. Sci. Lett., submitted, 1991.
25 W.B.F. Ryan, Stratigraphy of Late Quaternary sediments in the eastern Mediterranean, in: The Mediterranean Sea: A Natural Sedimentation Laboratory, D.J. Stanley, ed., Dowden, Hutchinson and Ross, Stroudsburg, Pa., pp. 146–169, 1972.
26 F.J. Hilgen, Sedimentary rhythms and high-resolution chronostratigraphic correlations in the Mediterranean Pliocene, Newslett. Stratigr. 17, 109–127, 1987.
27 R.B. Kidd, M.B. Cita and W.B.F. Ryan, The stratigraphy of eastern Mediterranean sapropel sequences as recovered by DSDP leg 42A and their paleoenvironmental significance, Init. Rep. DSDP 42A, 421–443, 1978.
28 R.C. Thunell, D.F. Williams and P.R. Belyea, Anoxic events in the Mediterranean Sea in relation to the evolution of Late Neogene climates, Mar. Geol. 59, 105–134, 1984.
29 P.J.J.M. Verhallen, Early development of *Bulimina marginata* in relation to paleoenvironmental changes in the Mediterranean, Proc. K. Ned. Akad. Wetensch., B 90, 161–180, 1987.
30 B.W.M. Driever, Calcareous nannofossil biostratigraphy and paleoenvironmental interpretation of the Mediterranean Pliocene, Utrecht Micropaleontol. Bull. 36, pp. 245, 1988.
31 F.J. Hilgen, Closing the gap in the Plio-Pleistocene boundary stratotype sequence of Crotone (southern Italy), Newslett. Stratigr. 22, 43–51, 1990.
32 A. Berger and M.F. Loutre, New insolation values for the climate of the last 10 Myr, Inst. Astron. Geophys. G. Lemaitre, Univ. Cathol. Louvain, Intern. Rep., 1988.
33 W.J. Zachariasse, L. Gudjonsson, F.J. Hilgen, C.G. Langereis, L.J. Lourens, P.J.J.M. Verhallen and J.D.A. Zijderveld, Late Gauss to early Matuyama invasions of *Neogloboquadrina atlantica* in the Mediterranean and associated record of climatic change, Paleoceanography 5, 239–252, 1990.
34 A. Berger, Long term variations of daily insolation and Quaternary climatic changes, J. Atmos. Sci. 35, 2362–2367, 1978.

35 N. Combourieu-Nebout, Les premiers cycles glaciaire–interglaciaire en region mediterranéenne d'après l'analyse palynologique de la série Crotone (Italie meriodionale), Thesis, Univ. Sci. Tech. Languedoc, Montpellier, 1987.
36 C. Vergnaud-Grazzini, M. Devaux and J. Znaidi, Stable isotope "anomalies" in Mediterranean Pleistocene records, Mar. Micropaleontol. 10, 35–69, 1986.
37 F.J. Jorissen, K. van der Borg, A.M. Borsetti, L. Gudjonsson, F.J. Hilgen, S. Iaccarino, A.F.M. de Jong, E.J. Rohling, J.P. de Visser and W.J. Zachariasse, Late Quaternary high-resolution biochronology for the central Mediterranean, Mar. Micropaleontol. in press, 1991.
38 W.L. Prell, Monssonal climate of the Arabian Sea during the late Quaternary; A response to changing solar radiation, in: Milankovitch and Climate, NATO ASI Ser. C, 126, A.L. Berger et al., eds., Reidel, Dordrecht, pp. 349–366, 1984.
39 D.A. Short and J.G. Mengel, Tropical climatic lags and Earth's precession cycle, Nature 323, 48–50, 1986.
40 A. McIntyre, W.F. Ruddiman, K. Karlin and A.C. Mix, Surface water response of the equatorial Atlantic Ocean to orbital forcing, Paleoceanography 4, 19–55, 1989.
41 W.F. Ruddiman, A. McIntyre and M. Raymo, Matuyama 41,000-year cycles: North Atlantic Ocean and northern hemisphere ice sheets, Earth Planet. Sci. Lett. 80, 117–129, 1986.
42 J.C. Davis, Statistics and data analysis in geology, Wiley, New York, 1973.
43 R.H. Steiger and E. Jager, Subcommision on geochronology: Convention on the use of decay constants in geo- and cosmochronology, Earth Planet. Sci. Lett. 36, 359–362, 1977.
44 F.J. Hilgen and C.G. Langereis, Periodicities of $CaCO_3$ cycles in the Mediterranean Pliocene: Discrepancies with the quasi-periods of the Earth's orbital cycles?, Terra Nova 1, 409–415, 1989.
45 A.L. Berger, Accuracy and frequency stability of the Earth's orbital elements during the Quaternary, in: Milankovitch and Climate, NATO ASI Ser. C, 126, A.L. Berger et al., eds., Reidel, Dordrecht, pp. 3–39, 1984.
46 M. Rossignol-Strick, African monsoons, an immediate climatic response to orbital insolation, Nature 303, 46–49, 1983.
47 C. Vergnaud-Grazzini, W.B.F. Ryan and M.B. Cita, Stable isotope fractionation, climatic change and episodic stagnation in the eastern Mediterranean during the Late Quaternary, Mar. Micropaleontol. 2, 353–370, 1977.
48 M.B. Cita, C. Vergnaud-Grazzini, C. Robert, H. Chamley, N. Ciaranfi and S. d'Onofrio, Paleoclimatic record of a long deep-sea record from the eastern Mediterranean, Quat. Res. 8, 205–235, 1978.
49 A. Murat and H. Got, Middle and Late Quaternary depositional sequences and cycles in the eastern Mediterranean, Sedimentology 34, 885–899, 1987.
50 Shipboard Scientific Party, Site 653, Proc. Init. Rep. (Pt. A) ODP 107, 599–745, 1987.
51 W.J. Zachariasse, J.D.A. Zijderveld, C.G. Langereis, F.J. Hilgen and P.J.J.M. Verhallen, Early Late Pliocene biochronology and surface water temperature variations in the Mediterranean, Mar. Micropaleontol. 14, 339–355, 1989.
52 M.B. Cita, Planktonic foraminiferal biozonation of the Mediterranean Pliocene deep sea record. A revision, Riv. Ital. Paleontol. Stratigr. 81, 527–544, 1975.
53 P. Spaak, Accuracy in correlation and ecological aspects of the planktonic foraminiferal zonation of the Mediterranean Pliocene, Utrecht Micropaleontol. Bull. 28, 1–160, 1983.
54 I. Raffi and D. Rio, Calcareous nannofossil biostratigraphy of DSDP Site 132-Leg 13 (western Mediterranean), Riv. Ital. Paleontol. Stratigr. 85, 127–172, 1979.
55 G. Glaçon, D. Rio and R. Sprovieri, Calcareous plankton Pliocene–Pleistocene biostratigraphy in the Tyrrhenian Sea (western Mediterranean, Leg 107), Proc. ODP, Sci. Results 107, 683–693, 1990.